

Magnetic thermal hysteresis in $\text{Fe}_m/\text{Dy}_n/\text{Fe}_m$ and $\text{Gd}_m/\text{Dy}_n/\text{Gd}_m$ trilayers

Ana L. Dantas* and R. E. Camley

Department of Physics, University of Colorado at Colorado Springs, Colorado Springs, Colorado 80918, USA

A. S. Carriço

Departamento de Física teórica e Experimental, Universidade Federal do Rio Grande do Norte, 59072-970, Natal-RN, Brazil

(Received 31 August 2006; published 30 March 2007)

We have performed a theoretical investigation of thermal hysteresis in the magnetization of $\text{Fe}_m/\text{Dy}_n/\text{Fe}_m$ and $\text{Gd}_m/\text{Dy}_n/\text{Gd}_m$ trilayers, where the interface coupling is antiferromagnetic and ferromagnetic, respectively. Our results show a large number of stable states can exist in these structures. The thermal hysteresis occurs because the transitions between these states occur at different temperatures for the heating and cooling processes. The thermal hysteresis can be quite large, spanning about 90 K. Furthermore the temperature span of the thermal hysteresis can be substantially reduced by applying a modest external magnetic field.

DOI: [10.1103/PhysRevB.75.094436](https://doi.org/10.1103/PhysRevB.75.094436)

PACS number(s): 75.25.+z, 75.10.-b, 75.30.Kz

I. INTRODUCTION

Despite the fact that thermal hysteresis is an old subject, there have been a number of recent studies showing thermal hysteresis in magnetic systems. This work has been stimulated by the fact that the thermal hysteresis in these new systems can be quite large (200 K) and can be tuned with modest external magnetic fields. The materials and systems have included experimental and theoretical studies of rare-earth and/or transition metal multilayers,^{1,2} experimental work on ferromagnetic-antiferromagnetic exchange bias structures,³ and experimental and theoretical work on alloys and compounds.^{4–6} Thermal hysteresis has been seen in neutron scattering measurements and in magnetization measurements.

Recently, we performed a theoretical study of thermal hysteresis in thin Dy films in the 80–179 K temperature interval.⁷ The results show that the thermal hysteresis originates in the combined effect of the strong temperature dependence of the magnetization of Dy and its hexagonal anisotropy and in surface effects. The thermal hysteresis could be quite large, covering the whole temperature interval between the Curie and the Néel temperatures, and could be strongly tuned by the external field.

In this paper, we theoretically investigate trilayers composed of a Dy film sandwiched between two films of Fe or Gd. The point of creating these trilayer structures is that by adding ferromagnetic films on the outside, one can further modify the effects of an external field on a Dy film. We note that the Fe is antiferromagnetically coupled to Dy at the interfaces, while Gd is ferromagnetically coupled to the Dy at the interfaces. This difference again allows substantial changes in how the external field interacts with the structure as a whole.

Magnetic configurations in Dy films and in other structures where Dy⁸ or other rare-earth helical magnets have been coupled to ferromagnets and other materials have been studied earlier by a variety of methods.^{9–13} However these works have concentrated primarily on magnetic structures and the phase transitions induced by magnetic fields and have not extensively looked at thermal hysteresis. We note

that recently there has also been an experimental report of thermal hysteresis in Cr/Cr_{97.5}Mn_{2.5} superlattices where the period of the spin density wave in the Cr showed a significant dependence on whether the sample was heated or cooled.¹⁴

One of the key factors in the recent studies of thermal hysteresis is that the thermal behavior of the different magnetic materials should be quite different. This is well satisfied by the combinations of Dy with Fe or Gd. At low temperatures the magnetic moment in Dy is $10\mu_B$ and goes to zero at 179 K while the magnetic moments of Fe and Gd, $2\mu_B$ and $7\mu_B$ at low temperature, respectively, are almost constant over the same temperature range.

We show in this paper that the thermal hysteresis in Fe/Dy/Fe or Gd/Dy/Gd is basically due to the helimagnetic nature of the Dy, combined with thickness, interface, and surface effects. For example, in Fe/Dy/Fe trilayers, where the Fe/Dy coupling is antiferromagnetic, we show that several states may participate in thermal hysteresis. At low temperatures there is an alternating-helix (AH) state where the Dy moments have one helicity in the first half of the Dy film and the opposite helicity in the second half of the film. At higher temperatures the stable state is an antiferromagnetic-like (AF) phase, where the magnetic moments of the Fe layers and of the middle planes of Dy are aligned with the magnetic field and the moment on the outer planes of the Dy film are antiparallel to the external field. When the system is heated or cooled there is a transition from one state to the other, but the transition temperature depends on the external field and whether one is heating or cooling. This difference in transition temperatures gives us the thermal hysteresis. The width of the thermal hysteresis can be quite large in this structure, typically around 90 K for low magnetic fields. As the thickness of the Fe is reduced, additional states such as a fan state or a ferrimagneticlike state also are involved in the thermal hysteresis.

We also study thermal hysteresis in Gd/Dy/Gd trilayers. In this case the Gd/Dy coupling is ferromagnetic and the states involved in the thermal hysteresis can be different from those described in the Fe/Dy/Fe trilayer structures.

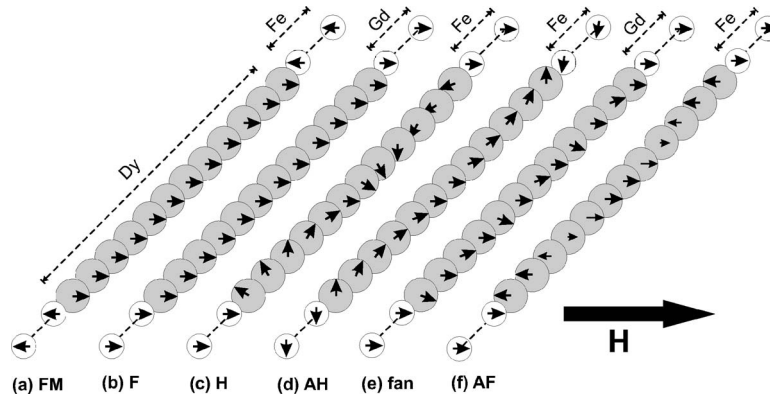


FIG. 1. (a) shows a ferrimagnetic-like (*FM*) configuration where the Dy moments are all aligned with the external field and the Fe are antiparallel. (b) shows a ferromagnetic (*F*) structure with all magnetic moments parallel to the applied field. (c) a structure where the Dy moments display a helical (*H*) structure as they do in a bulk material. (d) shows an alternating-helix (*AH*) structure where the direction of the helix reverses around the middle of the film. (e) shows a fan state which also has reversals of the helicity direction within the film, but allows the ends of the film to point along the external field. This state is particularly advantageous when Gd is on the outermost layers because then the Gd moments can also point along the external field, lowering the Zeeman energy. (f) shows an antiferromagneticlike (*AF*) state.

II. THEORY

We investigate the thermal hysteresis in $\text{Fe}_m/\text{Dy}_n/\text{Fe}_m$ and $\text{Gd}_m/\text{Dy}_n/\text{Gd}_m$ trilayers, where m is the number of ferromagnetic atomic planes (Fe or Gd) and n is the number of atomic planes of Dy. The xz plane is taken to coincide with the plane of each layer. The magnetic energy per unit area is proportional to

$$H = J_1(g-1)^2 \sum_{i=1}^{N-1} \vec{J}(i) \cdot \vec{J}(i+1) + J_2(g-1)^2 \sum_{\text{Dy}} \vec{J}(i) \cdot \vec{J}(i+2) + \sum_{\text{Dy}} K_6^6 \cos(6\phi_i) + \sum_{i=1}^N [2\pi(g\mu_B J_i^y)^2 - g\mu_B \vec{J}(i) \cdot \vec{H}], \quad (1)$$

where the magnetic moment per atom in the i th atomic layer is represented by a spin $\mathbf{S}(i) = (g-1)\mathbf{J}(i)$, where $\mathbf{J}(i)$ is the total angular momentum per atom. The spins are kept in the basal plane and ϕ_i is the angle with the easy axis. Each layer is exchange coupled with the first neighbor layers and second neighbor layers in the Dy. In Eq. (1) the first two terms represent the exchange energy, J_1 and J_2 are the exchange constant between first and second neighbors, respectively.

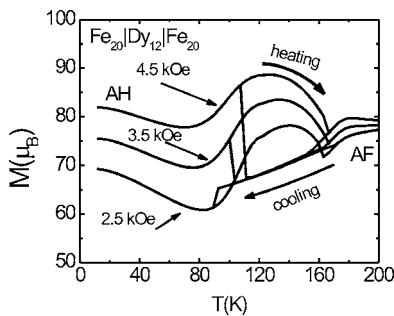


FIG. 2. Magnetization of trilayers of $\text{Fe}_{20}/\text{Dy}_{12}/\text{Fe}_{20}$ for both heating and cooling processes. Note the transitions and the thermal hysteresis are both tunable by a small external magnetic field.

The third term is the hexagonal anisotropy energy in the Dy. The temperature dependence is included by using the experimental value of the anisotropy constant K_6^6 . The anisotropy vanishes above $T=120$ K.⁸ The fourth and last term contains the demagnetizing and Zeeman energies. The external field is applied in the basal plane and along one of the easy directions in Dy, making an angle of 30° with the x axis.

For Dy we use $S=2.5$, $g=4/3$, corresponding to a total angular momentum $J=15/2$, and the nearest neighbor exchange is $J_1(\text{Dy})=44k_B$. The temperature dependence of the second neighbor exchange, $J_2(\text{Dy})=-J_1(\text{Dy})/4 \cos \phi(T)$, where the turn angle, $\phi(T)$, is a function of the temperature.¹⁵ For Fe, $g=2$, $S=J=1$, and the nearest neighbor exchange is $J_1(\text{Fe})=782k_B$. For Gd, $g=2$, $S=J=3.5$, and the nearest neighbor exchange is $J_1(\text{Gd})=156k_B$. We consider the interface coupling $J_{\text{int}}(\text{Gd}/\text{Dy})=J_1(\text{Dy})$ and $J_{\text{int}}(\text{Fe}/\text{Dy})=-J_1(\text{Dy})$. We note that bulk Dy undergoes a phase transition around 80 K and below this Dy is ferromagnetic. However Dy in a multilayer structure apparently is helimagnetic down to much lower temperatures^{10–12} and we use this assumption over the 15 K–180 K temperature interval studied here.

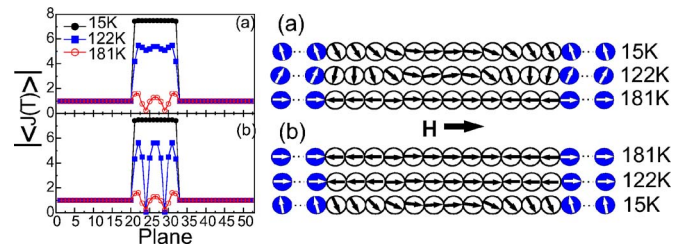


FIG. 3. (Color online) The left-hand panels show the absolute value of the thermally averaged total angular momentum by plane, for a trilayer $\text{Fe}_{20}/\text{Dy}_{12}/\text{Fe}_{20}$ in (a) heating and (b) cooling process in the presence of $H=2.5$ kOe. On the right-hand side we show the angular profiles for heating (a) and cooling (b). The filled circles represent the Fe layers, in the ferromagnetic phase, and the open circles represent the Dy layers.

The magnetic stability is calculated by the Landau-Lifshitz-Gilbert equation. This equation is the analogue of the classical equation $d\vec{L}/dt = \text{torque}$ and is given by

$$\frac{d\vec{M}_i}{dt} = \gamma_i \vec{M}_i \times \vec{H}_{\text{eff}}^i - \frac{\alpha_i \gamma_i}{M_i} \vec{M}_i \times (\vec{M}_i \times \vec{H}_{\text{eff}}^i), \quad (2)$$

where the first term on the right-hand side represents the torque on a magnetic moment due to an effective field \vec{H}_{eff}^i and the second term is a phenomenological damping term which allows relaxation of the magnetization toward the equilibrium direction (\vec{H}_{eff}^i) and keeps the length of the magnetization vector a constant in time. In Eq. (2) the magnetization, \vec{M}_i in layer i is coupled to the other layers through the effective field. The effective field can be found from the energy density using the usual relation

$$\vec{H}_{\text{eff}}^i = - \frac{\partial U}{\partial \vec{M}_i}. \quad (3)$$

This process produces a demagnetizing field $-4\pi M_y$ (in addition to the exchange field and applied field) which keeps the magnetization in the plane of the sample.

To obtain the spin configuration at a given temperature and field, one picks an initial spin configuration and integrates the coupled set of equations forward in time using a differential equation solver such as a fourth order Runge-Kutta method. To find the equilibrium position, a large value of the damping constant is used and one integrates forward in time until the M_i values do not change significantly. There is no guarantee that the final state is the ground state rather than some metastable state. One can then make small changes in temperature to trace out the behavior of the system during heating or cooling.

To take temperature into account we employ a local mean-field approximation. The thermal averaged magnetization in each layer is calculated using the Brillouin function

$$\langle M_i \rangle = M_i B_f(x), \quad (4)$$

where $B_f(x)$ is the Brillouin function and

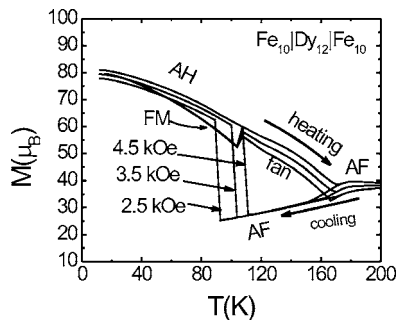


FIG. 4. Magnetization of trilayers of $\text{Fe}_{10}/\text{Dy}_{12}/\text{Fe}_{10}$, in thermal processes of heating and cooling in the presence of a magnetic field. The thermal hysteresis decreases as the field is increased.

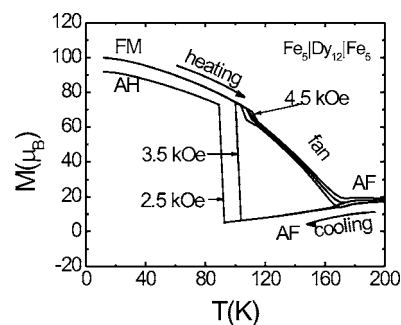


FIG. 5. Magnetization of trilayers $\text{Fe}_5/\text{Dy}_{12}/\text{Fe}_5$ for heating (filled symbols) and cooling (open symbols), in the presence of a magnetic field 2.5 kOe (circles), 3.5 kOe (squares), and 4.5 kOe (triangles).

$$x = \frac{\vec{M}_i \cdot \vec{H}_{\text{eff}}^i}{kT}. \quad (5)$$

Typically one may update the thermal magnitudes every few thousand time steps.

III. RESULTS

Before we investigate the thermal behavior of the magnetization, it is important to review some of the typical structures that occur in this system. Figure 1 illustrates some of the magnetic configurations that occur. Figure 1(a) shows a ferrimagneticlike (FM) configuration where the Dy moments are all aligned with the external field and the Fe are antiparallel to the field due to the antiferromagnetic exchange coupling at the interface. Figure 1(b) shows a ferromagnetic (F) configuration with all the magnetic moments parallel to the applied field. Figure 1(c) shows a structure where the Dy moments display a helical (H) structure as they do in a bulk material. Figure 1(d) shows an alternating-helix (AH) structure where the direction of the helix reverses around the middle of the film. In Fig. 1(e) a fan state also has a reversal of helicity direction within the film, but allows the ends of the film to point along the external field. This state is particularly advantageous when Gd is on the outermost layers because then the Gd moments can also point along the ex-

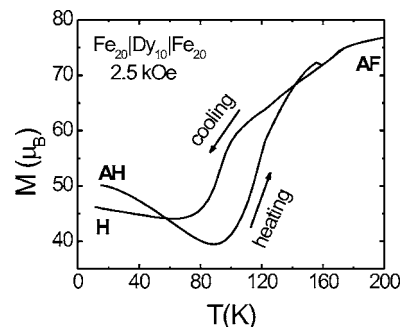


FIG. 6. Magnetization of trilayers $\text{Fe}_{20}/\text{Dy}_{10}/\text{Fe}_{20}$ for heating and cooling, in the presence of an applied field $H=2.5$ kOe. The low temperature state for the heating process is an AH state; the low temperature state for the cooling process is an H state.

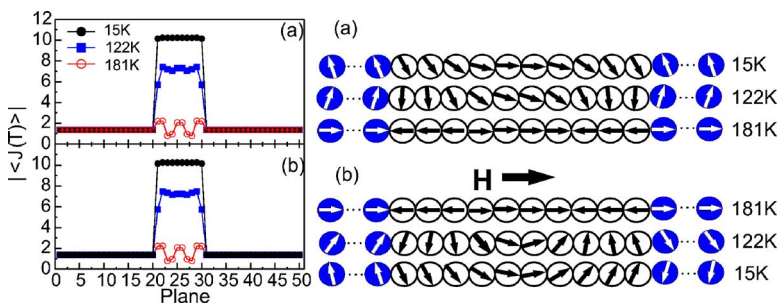


FIG. 7. (Color online) The left-hand panel shows the absolute value of the thermally averaged total angular momentum by plane, for a trilayer $\text{Fe}_{20}/\text{Dy}_{10}/\text{Fe}_{20}$ in (a) heating and (b) cooling in the presence of $H=2.5$ kOe. The right-hand side shows the angular profiles for $T=15$, 122, and 181 K. The filled circles represent the Fe layers, in a ferromagnetic state, and the open circles represent the Dy layers.

ternal field, lowering the Zeeman energy. The final state, an antiferromagneticlike state (*AF*), is shown in Fig. 1(f).

We now examine some of the results for the thermal behavior of the trilayer structures. In Fig. 2 we plot the magnetization as a function of temperature and for different magnetic fields for a $\text{Fe}_{20}/\text{Dy}_{12}/\text{Fe}_{20}$ structure. We see a clear thermal hysteresis in that the heating and cooling cycles give different results. To better understand the thermal hysteresis in this composition, we examine the evolution of magnetic structure in both heating and cooling in Fig. 3. On the left-hand side, we show the absolute value of the thermal average of the total magnetic moment, by plane, for both the heating and cooling processes. On the right-hand side we show the angular profile. We examine results at three temperatures $T=15$, 122, and 181 K. The ferromagnetic Fe layers are shown schematically as filled circles with the first and the last planes. The Dy layers are represented by open circles, in the center of the structure. We can see in the heating process that the magnetic phase of the Dy is in an alternating-helicity (*AH*) state where the helicity of the Dy film reverses at the center. [See Fig. 3(a), $T=15$ and 122 K.] At $T=163$ K there is a phase magnetic transition from *AH* to an *AF*-like state. In the cooling process the transition from the *AF*-like state to the *AH* state occurs at a different temperature. We can see that the thermal cycling involves hysteresis for both the thermally averaged magnetic moments (see left-hand side of Fig. 3), and for the angular orientation (see right-hand side of Fig. 3).

The width of the thermal hysteresis is tunable with applied magnetic field; it is about 90 K for a field of 2.5 kOe and decreases to 50 K at a field of 4.5 kOe. For weak external fields, $H=1.5$ kOe, the initial configuration at low temperatures is not recovered after both heating and cooling. For a strong external magnetic field, $H=5.5$ kOe, there is no hysteresis.

We now explore the phases and thermal behavior in the $\text{Fe}_{10}/\text{Dy}_{12}/\text{Fe}_{10}$ structure where the number of Fe layers has been reduced by a factor of 2 from the previous case. The magnetization as a function of temperature is shown in Fig. 4. The main difference from the earlier case is that a new *FM* state now occurs at low temperatures. In this state the Dy are all aligned parallel to the external field and the Fe are all antiparallel. Such a state is energetically unfavorable in the $\text{Fe}_{20}/\text{Dy}_{12}/\text{Fe}_{20}$ structure because the large number of Fe spins opposite to the external field is costly in terms of Zeeman energy; however when the number of Fe spins is reduced, this state becomes stable.

A further reduction in the thickness of the Fe layer, to $\text{Fe}_5/\text{Dy}_{12}/\text{Fe}_5$, again reduces the importance of the Zeeman

energy of the Fe. The magnetization curves for this structure are shown in Fig. 5. As a result of making the Fe thinner, another new state occurs, the fan state. We will see that this state occurs in a Dy_{12} film by itself, so what has happened is that the Fe film thickness has now been reduced sufficiently so that the magnetic structure is primarily determined by the Dy film alone. Despite these changes, many of the features of the thermal hysteresis seen in the earlier examples remain unchanged.

The magnetic phases of the trilayer structure are extremely sensitive to the Dy thickness because the turn angle from one Dy plane to the next can be quite large, typically 30° to 50° . Because of the large Fe films at the ends of the Dy, changes in turn angle can make substantial changes in the magnetization and resulting structure. This is illustrated in Fig. 6, which shows the magnetization versus temperature for the $\text{Fe}_{20}/\text{Dy}_{10}/\text{Fe}_{20}$ trilayer, for $H=2.5$ kOe. The results are completely different from the $\text{Fe}_{20}/\text{Dy}_{12}/\text{Fe}_{20}$ case (see Fig. 2). The reason for this is that for thin Dy layers the average magnetic moment in each plane is almost constant, stabilized by contact with the Fe. (See Fig. 7.) This is in sharp contrast with the $\text{Fe}_{20}/\text{Dy}_{12}/\text{Fe}_{20}$ case, where the magnetic moment oscillates in magnitude from plane to plane. This large and constant magnetic moment in the Dy favors a helimagnetic state, and the *AF*-like phase, prominent in the $\text{Fe}_{20}/\text{Dy}_{12}/\text{Fe}_{20}$ structure, now vanishes below 160 K. The details of the structure are shown in Fig. 7.

Trilayers of $\text{Gd}/\text{Dy}/\text{Gd}$, where the interface coupling is ferromagnetic, emphasize the role of the Zeeman interaction. As a result, the Gd layers tend to be aligned or only slightly canted with respect to the direction of the external magnetic field. We examine the temperature dependence of the magnetization for a $\text{Gd}_{10}/\text{Dy}_{12}/\text{Gd}_{10}$ structure in Fig. 8. In the

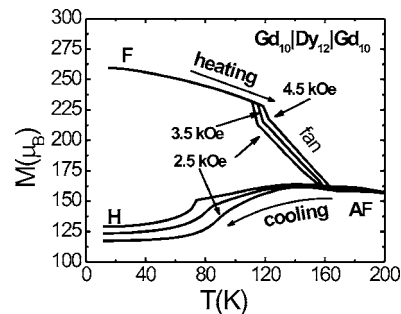


FIG. 8. Magnetization of trilayers $\text{Gd}_{10}/\text{Dy}_{12}/\text{Gd}_{10}$ for heating and cooling, in the presence of $H=2.5$ kOe. The initial state is a low temperature ferromagnetic state and the system is heated and then cooled.

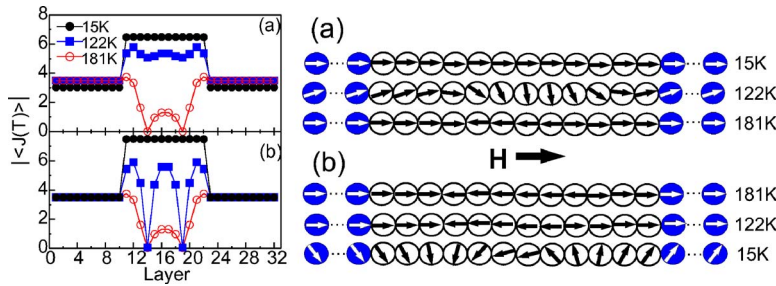


FIG. 9. (Color online) The left-hand panel shows the absolute value of the thermally averaged total angular moment for the $\text{Gd}_{10}/\text{Dy}_{12}/\text{Gd}_{10}$ trilayer with (a) heating and (b) cooling in the presence of $H=2.5$ kOe. The right-hand side shows the angular profile again with (a) heating and (b) cooling. The filled circles represent the Fe layers, in the ferromagnetic phase, and the open circles represent the Dy layers.

heating process the states go from ferromagnetic to fan to AF as the temperature is increased. In the cooling process the states progress from the AF state to the full helix state. The heating process favors a structure at low temperature where the magnetic moment of the Gd and Dy layers are along the direction of the external magnetic field [see Fig. 9(a)]. After the cooling thermal process, the magnetic moments of Gd layers are in the direction of the external field, but the moments in the center of the Dy are nearly antiparallel to the external magnetic field. This loss in Zeeman energy is compensated by the helical structure which has the lowest exchange energy. We can see in Fig. 8 that the initial low temperature state is not recovered after both heating and cooling. The structure $\text{Gd}_{20}/\text{Dy}_{12}/\text{Gd}_{20}$ has a qualitatively similar set of magnetization curves as those seen in Fig. 8 for $\text{Gd}_{10}/\text{Dy}_{12}/\text{Gd}_{10}$.

It is interesting to compare the magnetization curves of a thin Dy film to those seen for the multilayer structures. Figure 10 shows the results for a single Dy_{12} film at an external field of 2.5 kOe. There are three states which occur—ferromagnetic, fan, and AF . Although there are small thermal hysteresis loops at each of the phase transitions, the major results are quite different from what is seen in Fig. 8, for example.

At first glance, it is surprising that the helical phase occurs when Gd films are on the outside of the Dy film, but the helical phase does not occur for the pure Dy film for external fields of 2.5 kOe or above. The explanation for this starts with the fact that the system is in an AF state at high temperatures. Such a state has a built-in twist which can evolve naturally into the helical state as the temperature is lowered. If there are no Gd films on the outside of the Dy, however, the helical state can unwind and have all the spins pointing along the field. This unwinding involves a full rotation of the

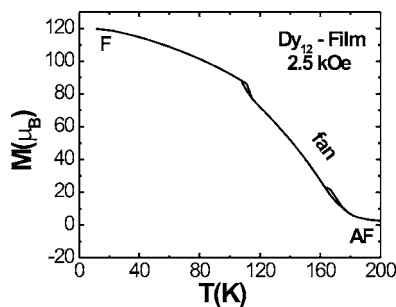


FIG. 10. Magnetization curves for a 12 layer Dy film showing three phases and small thermal hysteresis between the different phases.

outermost layers. In contrast, when the Gd spins are present, it is difficult for the outer layers and the Gd layers to unwind because the full rotation is too costly in Zeeman energy. As a result, the $\text{Gd}_{10}/\text{Dy}_{12}/\text{Gd}_{10}$ system goes from the AF phase to the helical phase, but the pure Dy_{12} film can go into a low temperature ferromagneticlike phase.

As a final example, we present the magnetization as a function of temperature for a $\text{Gd}_5/\text{Dy}_6/\text{Gd}_5$ trilayer in Fig. 11. At low temperatures, the system is ferromagnetic. Upon heating, the system jumps into a canted phase which eventually resembles the AF phase at the highest temperatures. When cooled from high temperatures, the system has a continuous transformation from the canted phase which eventually merges into the ferromagnetic phase. We note that the naming of the canted phase is somewhat arbitrary. In these thin film systems there are no phases with infinite translational periodicity. So, the canted phase could equally well be called a modified helical phase in a very thin film.

In summary, we have performed theoretical calculations for structures composed of ferromagnets and helical rare-earth magnets. Our results show that $\text{Fe}/\text{Dy}/\text{Fe}$ and $\text{Gd}/\text{Dy}/\text{Gd}$ structures have a number of magnetic phases and that transitions from one phase to another can be easily accomplished by moderate changes in an external magnetic field. Furthermore, changes in temperature may also result in phase changes, but these changes are not directly reversible, leading to thermal hysteresis. We find that the thermal hysteresis can span about 90 K at low magnetic fields and can be reduced as the external field is increased.

We comment on some of the limitations of the model. First, the model is essentially a one-dimensional chain and

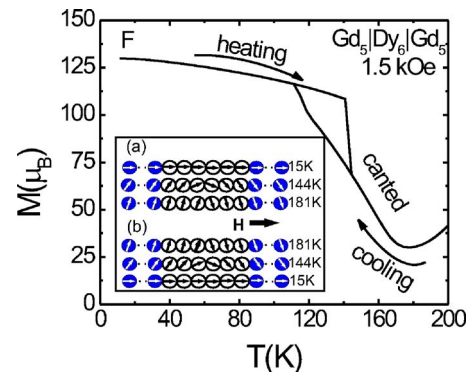


FIG. 11. (Color online) Magnetization of trilayers of $\text{Gd}_5/\text{Dy}_6/\text{Gd}_5$ for both heating and cooling processes. Heating (filled circles) and cooling (opened circles) are done in the presence of $H=1.5$ kOe. The inset shows the angular profile for (a) heating and (b) cooling.

because of this phase changes from one state to another do not include mechanisms which might involve lateral inhomogeneities, i.e., nucleation and domain reversal. Nonetheless, similar one-dimensional models have given a good account of phase changes measured in other helical-ferromagnetic¹⁰ and ferromagnetic-ferromagnetic multilayer structures.⁹ Similarly we note that the system can be quite sensitive to slight variations in thickness as evidenced by the results when the Dy is 10 or 12 layers thick. However, layer-by-layer growth is possible using molecular beam epitaxy and structures which are very sensitive to thickness variations have been grown and studied. One very

successful experimental method has been to produce samples with a film in the form of a wedge. For example, in the Fe/Cr multilayers one can see alternations in the exchange coupling which arise from adding a single Cr layer.¹⁶

ACKNOWLEDGMENTS

This research was partially supported by the CAPES and CNPq. This work was also supported by DOA Grant No. W911NF-04-1-0247 and U.S. ARO Grant No. DAAD19-02-1-0174. R.E.C. would like to thank S. D. Bader for a stimulating discussion which helped motivate this work.

*Permanent address: DCC, Universidade do Estado do Rio Grande do Norte, 59124-400, Natal-RN, Brazil. Electronic address: anadantas@uern.br

¹R. E. Camley, W. Lohstroh, G. P. Felcher, N. Hosoi, and H. Hashizume, *J. Magn. Magn. Mater.* **286**, 65 (2005).

²S. Demirtas, M. R. Hossu, R. E. Camley, H. C. Mireles, and A. R. Koymen, *Phys. Rev. B* **72**, 184433 (2005).

³Zhi-Pan Li, Johannes Eisenmenger, Casey W. Miller, and Ivan K. Schuller, *Phys. Rev. Lett.* **96**, 137201 (2006).

⁴S. Maat, J.-U. Thiele, and Eric E. Fullerton, *Phys. Rev. B* **72**, 214432 (2005).

⁵J. Dho, W. S. Kim, and N. H. Hur, *Phys. Rev. Lett.* **87**, 187201 (2001).

⁶S. Demirtas, R. E. Camley, and A. R. Koymen, *Appl. Phys. Lett.* **87**, 202111 (2005).

⁷Ana L. Dantas, R. E. Camley, and A. S. Carriço, *IEEE Trans. Magn.* **42**, 2942 (2006).

⁸J. J. Rhyne and A. E. Clark, *J. Appl. Phys.* **38**, 1379 (1967).

⁹R. E. Camley and R. L. Stamps, *J. Phys.: Condens. Matter* **5**,

3727 (1993).

¹⁰R. E. Camley, J. Kwo, M. Hong, and C. L. Chien, *Phys. Rev. Lett.* **64**, 2703 (1990).

¹¹C. Dufour, K. Dumesnil, A. Mougou, Ph. Mangin, G. Marchal, and M. Hennion, *J. Phys.: Condens. Matter* **9**, L131 (1997).

¹²C. F. Majkrzak, Doon Gibbs, P. Böni, Alan I. Goldman, J. Kwo, M. Hong, T. C. Hsieh, R. M. Fleming, D. B. McWhan, Y. Yafet, J. W. Cable, J. Bohr, H. Grimm, and C. L. Chien, *J. Appl. Phys.* **63**, 3447 (1988).

¹³J. Jensen and A. R. Mackintosh, *Phys. Rev. Lett.* **64**, 2699 (1990).

¹⁴E. E. Fullerton, J. L. Robertson, A. R. E. Prinsloo, H. L. Alberts, and S. D. Bader, *Phys. Rev. Lett.* **91**, 237201 (2003).

¹⁵M. K. Wilkinson, W. C. Koehler, E. O. Wollan, and J. W. Cable, *J. Appl. Phys.* **32**, S48 (1961).

¹⁶J. Unguris, R. J. Celotta, and D. T. Pierce, *Phys. Rev. Lett.* **67**, 140 (1991).